Composite spectra Paper 15: HD 216572, a triple system containing a short-period, double-lined secondary

Griffin, R. E. M.; Griffin, R. F.

Publisher's version / Version de l'éditeur:
https://doi.org/10.1111/j.1365-2966.2008.14133.x
Monthly Notices of the Royal Astronomical Society, 394, 3, pp. 1393-1408, 2009-04-03

NRC Publications Record / Notice d'Archives des publications de CNRC:
https://nrc-publications.canada.ca/eng/view/object/?id=17fc469e-4fd1-4b16-a558-c112c846ca32
https://publications-cnrc.canada.ca/fra/voir/objet/?id=17fc469e-4fd1-4b16-a558-c112c846ca32

Mon. Not. R. Astron. Soc. **394,** 1393–1408 (2009) doi:10.1111/j.1365-2966.2008.14133.x

Composite spectra
Paper 15: HD 216572, a triple system containing a short-period, double-lined secondary

R. E. M. Griffin[1]★† and R. F. Griffin[2]†

[1]*Herzberg Institute of Astrophysics, National Research Council, 5071 West Saanich Road, Victoria, BC, V9E 2E7, Canada*
[2]*The Observatories, Institute of Astronomy, Madingley Road, Cambridge CB3 0HA*

Accepted 2008 October 20. Received 2008 October 20; in original form 2008 May 30

ABSTRACT

We analyse 81 optical spectra of the composite-spectrum binary HD 216572, and show that the primary is a cool giant of type G8 III while the secondary is a double-lined binary consisting of two nearly identical B9 dwarfs in a 1.18-d orbit. The inner system undergoes partial eclipses, whose photometry we model to derive the physical parameters of both secondary stars. The outer system does not eclipse. We isolate the combined spectrum of the secondary by spectral subtraction, and from 48 separate radial-velocity measurements of both secondary components we obtain a triple-lined orbit solution from which we determine the individual masses of all three stars and the inclinations of both the inner and the outer orbits. The period of the outer system is 55 d, which is surprisingly short for a giant star, and our detection of small but non-negligible amounts of variable chromospheric emission in the Ca II K line is not unlike that detected in other systems with comparably short periods. The secondary components are in a circular orbit and are rotating at about 95 ± 10 km s^{-1}; although their surface-to-surface separation is only 4 $R_\odot$ the stars are not noticeably distorted geometrically by such close proximity. All three stars appear to be in synchronous rotation in their respective orbits. We derive fairly accurate Hertzsprung–Russell diagram positions for all three stars and compare them to evolutionary tracks calculated for the respective stellar masses, but cannot reconcile the age of the cool giant with that of the B stars.

Key words: binaries: spectroscopic – stars: evolution – stars: individual: HD 216572.

1 INTRODUCTION

Composite-spectrum binaries, which by definition have components that are of dissimilar spectral types and are thus at different stages of evolution, constitute an important resource through the ready opportunities they provide to determine the mass ratios of their component stars. The knowledge thus gained furnishes much-needed constraints for stellar-evolution theory, while at the same time any model of the binary must itself meet the basic requirement that the evolutionary ages of the components be similar. Determining the mass ratios of composite-spectrum binaries has even acquired some urgency owing to the notorious uncertainties attached to the derivation of the masses of single evolved stars. Many composite-spectrum binaries also prove to be of considerable astrophysical interest in their own right, and the subject of this paper (HD 216572) is a case in point. It is the first object that we have analysed in this series in which the secondary is itself a double-lined spectroscopic binary (though it is not a composite-spectrum one), while the cool-giant primary shows evidence of rather rapid rotation and some chromospheric activity.

HD 216572 appears as a 7.5-mag star in a conveniently circumpolar location ($\delta \sim 61^\circ$) for observation from northern temperate latitudes – it is $\sim 4^\circ$ north-following δ Cephei, and a little more than a degree north of the Galactic equator. It is also the brighter star of a visual double. Attention was drawn to that fact by Struve (1827), who was the first to catalogue it as a double star. It retains his designation, Σ 2953, and is also known as ADS 16334 from its entry in Aitken (1932)'s double-star catalogue. However, the HD designation refers only to the brighter component, which alone is the subject of this paper.

Blanco et al. (1955) determined the spectral type of HD 216572 as A2m from objective-prism plates. One of those authors (Nassau), benefiting later from higher-dispersion slit spectra, described it as showing 'an A-type K line plus the G band characteristic of composite spectra' (Slettebak & Nassau 1959). The HD type (Cannon & Pickering 1924) is A0. Kuhi (1963) found the cool component of HD 216572 to be G0 III; Abt (1985) gave the spectral type of the system as A0: V + G0: III.

★Guest Worker.
†E-mail: Elizabeth.Griffin@nrc.gc.ca (REMG); rfg@ast.cam.ac.uk (RFG)

Struve considered the components of the visual double star to be of magnitudes 7.5 and 9.5, and measured the secondary as being 8.29 arcsec from the primary in position angle 137°.7 (Struve 1837). It says as much for Struve's observational acumen as for the relative fixity of the components that the modern measurement by *Hipparcos* (ESA 1997, vol. 10, p. DC432) yielded the corresponding quantities as 8.39 arcsec and 137°.7. As the proper motion measured by *Hipparcos* for the primary star would have carried it some 2 arcsec across the sky since Struve's time, the lack of relative movement is strong evidence of true physical association.

In the main part of the *Hipparcos* catalogue (vol. 9, pp. 2268/9) HD 216572 is listed as having a V magnitude, determined by *Hipparcos* itself, of 7.42, and a $(B - V)$ colour index, derived from *Tycho* V_T and B_T magnitudes by the transformations given by equations 1.3.20 (vol. 1, p. 57), of 0.529 ± 0.029 mag. All measurements included the light of the visual companion, which contributes ~9 per cent of the total light; the H_P magnitudes of the components of the visual double system are given separately in the 'double and multiple systems annex' of the *Hipparcos* catalogue (vol. 10, p. DC432) as 7.653 ± 0.006 and 10.163 ± 0.053, i.e. $\Delta H_P = 2.51 \pm 0.06$, implying after transformation $\Delta V = 2.45$, whereas the respective *Tycho* V_T magnitudes of 7.617 ± 0.008 and 9.521 ± 0.134 yield $\Delta V = 1.85$ mag, a discrepancy that is more than four times greater than the formal errors allow. The magnitudes quoted by the CDS, though obtained through the same transformations, differ slightly from our own, while the revised *Tycho-2* catalogue (Høg et al. 2000) gives magnitudes for the primary that are slightly different again, but it does not mention the visual secondary. Our present analysis actually incorporates unpublished photometry for the combined system (see Sections 3 and 7.1) in combination with the *Hipparcos* ΔV.

The only published ground-based photoelectric photometry of HD 216572 is that of Blanco et al. (1955), who happened to select it as a standard for photographic cluster photometry. They give $V = 7.50$, $B - V = 0.52$ mag.

2 RADIAL VELOCITIES AND ORBIT

No individual radial-velocity (RV) measurements have been published previously for HD 216572. One of the present authors published preliminary orbital elements for the late-type component (Griffin 1990), without giving any data and with only the briefest – and, as we now recognize, quite erroneous – discussion. An electronic table of velocities mentioned by Grenier et al. (1999) merely states that four RVs had been obtained and that they show the velocity to be variable; the spectral type is quoted there as A0 Vp.

In Table 1 we list 130 RV measurements that we have now made: 67 with the Geneva Observatory's Coravel at Haute-Provence (Baranne, Mayor & Poncet 1979), 37 with the original Cambridge spectrometer (Griffin 1967), 22 with its replacement Coravel-type one, three with the Dominion Astrophysical Observatory (DAO) spectrometer (Fletcher et al. 1982) at the 48-inch telescope, and one with the Palomar 200-inch telescope and spectrometer (Griffin & Gunn 1974). Dr S. Udry has kindly reduced the Haute-Provence observations, using the post-2000 zero-point (Udry, Mayor & Queloz 1999); to place those observations on the same scale as the others, which were reduced to the Cambridge zero-point through the use of specified reference stars (Griffin 1969), an empirical adjustment of $+0.8$ km s^{-1} has been applied – the adjustment is already made in the entries given in Table 1.

Most of the velocities upon which the orbit is based have been attributed the same (unit) weight, but those obtained with the original Cambridge spectrometer are somewhat more ragged than the others and have needed to be attributed a one-third weight. Three measurements made with the Cambridge Coravel in 1992, when it was in a very preliminary form, have been similarly treated. All the later Cambridge measures have been adjusted by -0.2 km s^{-1} from the 'as initially reduced' values, an amount that is in keeping with the zero-point offset found in other cases of stars with similar colour indices, e.g. Griffin (2006). The 14 measurements obtained in 2006 had increased integration times and yielded much smaller residuals than any of the previous observations; they were double-weighted in the orbit solution.

A tabulation of the orbital elements is deferred until after we have described the measurements of the secondary component and can present a double-lined solution (Section 6.2 and Table 4). We refer here, however, to the calculation of the orbit of the primary star (the late-type giant), because all RVs of the secondary were determined in the rest frame of the primary, whose absolute velocity needed to be known at each relevant epoch in order to place the velocities of the secondary on an absolute scale. For that purpose the primary's RVs were determined from an orbit computed for it on a stand-alone basis. That orbit is, however, practically the same as was subsequently obtained from the double-lined solution (in which the elements of the primary's orbit were again allowed as free parameters), because the relatively very small standard errors of the primary RVs implied that those data carried the great majority of the weight in the overall solution.

The only decision that needed to be made in connection with the calculation of the orbit was whether or not to deem it to be exactly circular. When the eccentricity was allowed to take its optimum value, that value was 0.0043 ± 0.0016 – very small, but nevertheless approaching three times its own standard error. The question of its significance was decided on the basis of Bassett (1978)'s second statistical test, which yielded a significance level of $2\frac{1}{2}$ per cent, so we concluded that the eccentricity is 'probably significant' at that level, and we have accordingly adopted the eccentric solution.

The 'dips' in the RV traces are very shallow (about 8 per cent of the 'continuum') and considerably broadened, presumably by stellar rotation. Dilution of the late-type spectrum by the hot continuum arising from the B stars reduces the equivalent width of the dips to scarcely one-third of the norm for late-type giant stars. It is the shallow and wide character of the dip that is responsible for the indifferent precision of the measured RVs, the rms residual for an observation of unit weight being 0.87 km s^{-1}. The rotational velocity derived from the mean width of the dip given by the Haute-Provence Coravel is 14.3 km s^{-1}, with a formal standard error of 0.3 km s^{-1}, although a true uncertainty less than 1 km s^{-1} is never claimed for such results. The corresponding value from the Cambridge traces is 14.0 ± 0.2 km s^{-1}.

3 BINARY NATURE OF THE SECONDARY

An arresting feature of the orbital elements derived from the single-lined orbit is the extraordinary mass function of 2.14 $M_\odot$. The reason why it is so large is that the spectroscopic secondary is itself a double star. In his note on HD 216572, Griffin (1990) remarked that the mass function 'can hardly be due to duplicity of the secondary, since the period of the observed orbit is too short to admit of it', thus implicitly accepting mass exchange as the explanation and dismissing what has actually proved to be the true case. Certainly the period of only 55 d is already very short for a giant star, and although one triple system, λ Tau, is known with a 'long' period of only 33 d (Schlesinger 1914; Fekel & Tomkin 1982), that system is

Table 1. Radial-velocity observations of the giant component of HD 216572.
Except as noted, the sources of the observations are as follows: 1986–90 – original Cambridge spectrometer (Griffin 1967) (weight 1/3 in orbital solution); 1991–98 – Haute-Provence Coravel (Baranne et al. 1979) (weight 1); 2006 – Cambridge Coravel (weight 2).

Date (UT)	MJD	Velocity km s^{-1}	Phase	(O − C) km s^{-1}
1986 Oct. 20.95	46723.95	+57.7	0.575	−1.6
30.96	733.96	+3.9	.758	+0.3
Nov. 24.15*	758.15	−49.9	1.200	−0.3
Dec. 6.89	770.89	+45.8	.433	+0.4
1987 Mar. 5.81†	46859.81	−86.1	3.058	−2.9
May 5.05	920.05	−62.7	4.159	+1.4
9.06	924.06	−34.5	.232	+2.0
June 23.05	969.05	−84.0	5.055	−0.6
July 3.99	979.99	−28.2	.254	−1.4
5.07	981.07	−18.5	.274	−0.6
6.07	982.07	−8.4	.292	+1.3
Sept. 15.01	47053.01	+58.2	6.589	+0.5
24.95	062.95	−4.2	.771	−2.2
26.94	064.94	−17.4	.807	+1.1
Oct. 6.91	074.91	−84.4	.989	−4.3
12.79†	080.79	−78.1	7.097	+1.0
12.97†	080.97	−78.4	.100	+0.1
13.19†	081.19	−78.0	.104	−0.2
13.78†	081.78	−76.9	.115	−1.2
17.15†	085.15	−59.5	.176	−1.1
17.94†	085.94	−52.1	.191	+1.1
18.78†	086.78	−48.0	.206	−0.7
21.79	089.79	−25.8	.261	−2.0
22.83	090.83	−15.2	.280	+0.1
24.81	092.81	+0.9	.316	−0.2
28.79	096.79	+28.6	.389	−2.5
Nov. 20.79	119.79	−21.8	.809	−2.2
27.77	126.77	−69.0	.937	−0.1
Dec. 7.74	136.74	−75.1	8.119	−0.3
31.88	160.88	+59.6	.560	−0.8
1988 Jan. 26.13‡	47186.13	−82.5	9.022	+0.8
Feb. 1.09‡	192.09	−72.8	.131	−0.8
Mar. 12.80†	232.80	−48.2	.875	−0.5
June 23.07	335.07	+8.8	11.744	−1.1
July 27.08	369.08	+25.0	12.365	+3.0
Aug. 29.10	402.10	−78.1	.969	−1.5
Sept. 12.02	416.02	−39.1	13.223	+1.2
Oct. 10.94	444.94	+5.1	.752	−1.3
Nov. 2.89†	467.89	−60.1	14.171	0.0
3.93†	468.93	−53.5	.190	−0.1
6.94†	471.94	−29.1	.245	+1.8
Dec. 5.95	500.95	−3.7	.775	+0.4
12.82	507.82	−55.7	.901	+1.8
1989 Jan. 12.80	47538.80	+52.6	15.467	−1.0
16.76	542.76	+60.9	.539	−0.1
Apr. 28.14†	644.14	+32.6	17.392	+0.3
May 3.13†	649.13	+54.8	.483	−1.7
Oct. 17.96	816.96	+58.6	20.551	−2.2
27.96†	826.96	+13.3	.733	−1.1
29.82†	828.82	−0.8	.767	−0.3
Nov. 1.83†	831.83	−25.9	.822	−0.4
25.85	855.85	−22.8	21.261	+0.9
29.77	859.77	+6.0	.333	−2.5
Dec. 22.80	882.80	+7.1	.754	+1.6
1990 Jan. 30.76†	47921.76	+53.5	22.466	+0.2
July 15.08	48087.08	+55.3	25.487	−1.7
19.02	091.02	+61.0	.559	+0.5
Oct. 7.00	171.00	−82.9	27.021	+0.3
1991 Jan. 26.82	48282.82	−81.0	29.065	+1.8
29.75	285.75	−74.5	.118	+0.5
Oct. 29.91	558.91	−77.1	34.110	−0.5
31.92	560.92	−68.1	.147	−0.4
Nov. 1.91	561.91	−61.9	.165	+0.2
Dec. 16.80	606.80	−78.6	.986	+0.9
17.80	607.80	−81.9	35.004	0.0
18.81	608.81	−83.4	.022	−0.1
19.91	609.91	−84.1	.042	−0.4
21.81	611.81	−80.0	.077	+1.7
1992 Jan. 13.74	48634.74	+59.2	35.496	+1.0
14.76	635.76	+59.5	.515	−0.5
15.74	636.74	+60.2	.533	−0.7
16.75	637.75	+59.6	.551	−1.2
17.74	638.74	+60.2	.569	+0.4
18.76	639.76	+58.0	.588	+0.2
19.74	640.74	+55.1	.606	+0.1
22.73	643.73	+42.1	.660	+0.5
Apr. 21.82	733.82	−5.1	37.307	−2.0
June 21.09	794.09	+38.3	38.408	+0.5
26.07	799.07	+58.6	.499	0.0
Aug. 13.05	847.05	+26.6	39.376	+0.3
15.03	849.03	+37.2	.412	−2.0
Nov. 11.96§	937.96	−83.1	41.038	+0.6
17.78§	943.78	−71.6	.144	−3.1
26.80§	952.80	−3.0	.309	−0.8
Dec. 17.76	973.76	+31.1	.692	+0.2
21.78	977.78	−0.2	.765	−0.6
1993 Feb. 13.77	49031.77	+5.6	42.752	−0.7
July 7.08	175.08	+24.3	45.371	0.0
9.09	177.09	+37.5	.408	−0.2
11.10	179.10	+49.0	.445	+0.5
1994 Jan. 3.81	49355.81	+38.5	48.674	+1.4
4.76	356.76	+32.8	.692	+1.8
Aug. 3.02	567.02	+60.8	52.534	−0.1
Dec. 10.80	696.80	−59.2	54.906	+0.1
12.82	698.82	−69.9	.943	+0.7
13.84	699.84	−74.1	.962	+1.0
27.79	713.79	−41.9	55.217	+1.2
1995 Jan. 1.82	49718.82	−1.2	55.308	+1.2
3.77	720.77	+14.8	.344	+1.6
Dec. 21.81	50072.81	−4.9	61.778	+0.4
26.85	077.85	−45.0	.870	+0.8
1996 Nov. 18.86¶	50405.86	−44.4	67.865	−0.8
Dec. 4.82¶	421.82	−65.4	68.156	−0.5
23.75	440.75	+59.7	.502	+0.8
1997 Jan. 25.73	50473.73	−77.5	69.105	+0.1
May 10.10¶	578.10	−82.1	71.012	+0.6
July 19.08	648.08	−9.5	72.291	+0.7
21.06	650.06	+6.1	.327	+0.1
Sept. 9.95	700.95	−26.1	73.258	−0.7
Dec. 23.79	805.79	−60.1	75.174	−0.8
1998 July 9.06	51003.06	−5.8	78.779	−0.1
15.09	009.09	−52.8	.889	+0.4
24.08	018.08	−82.4	79.053	+1.1
1999 July 10.41‡	51369.41	+54.6	85.474	−0.3
Dec. 19.82¶	531.82	+48.1	88.442	+0.2
2000 Jan. 8.77¶	51551.77	−17.8	88.807	+0.6
2006 July 25.09	53941.09	+55.0	132.473	+0.3
Sept. 11.05	989.05	+16.0	133.350	+0.4
19.94	997.94	+59.9	.512	0.0
22.98	54000.98	+60.4	.568	+0.5
26.89	004.89	+47.7	.639	+0.1
30.88	008.88	+23.8	.712	+0.7
Oct. 5.04	013.04	−10.7	.788	−0.7
7.88	015.88	−33.7	.840	−0.4
21.89	029.89	−79.4	134.096	−0.2
24.97	032.97	−66.5	.152	−0.4
31.88	039.88	−15.8	.279	+0.1
Dec. 3.78	072.78	−49.8	.880	0.0
8.94	077.94	−77.5	.974	+0.1
11.90	080.90	−83.6	135.028	0.0

*Observed with Palomar 200-inch telescope (weight 1)
†Observed with Haute-Provence Coravel (weight 1)
‡Observed with DAO 48-inch telescope (weight 1)
§Observed with Cambridge Coravel (weight 1/3)
¶Observed with Cambridge Coravel (weight 1)

Table 2. Photometric observations of HD 216572. The original values, contributed by different amateur observers as noted in Section 3, were made with respect to the reference star HD 216380; they were converted to absolute values by adopting the magnitudes $V = 5.60$, $(B - V) = 0.78$, $(U - B) = 0.39$ for that star.

JD − 244 0000	V	B	U	JD − 244 0000	V	B	U	JD − 244 0000	V	B	U
7825.448§	7.404			7849.630*	7.421	7.927	8.078	8093.788†	7.439	7.955	8.118
7841.712*	7.459			7849.632*	7.425			8124.702†	7.427	7.934	8.113
7841.715*	7.470			7849.633*	7.427	7.935	8.085	8124.706†	7.440	7.950	8.102
7841.716*	7.460	7.992	8.152	7849.635*	7.425	7.926	8.084	8125.709†	7.443	7.953	8.120
7841.717*	7.479			7854.667‡	7.445			8125.723†	7.429	7.953	8.115
7841.718*	7.470	7.997	8.190	7855.493‡	7.449			8125.728†	7.437	7.943	8.107
7841.720*	7.478	8.005	8.194	7857.538‡	7.450			8125.730†	7.431	7.956	8.102
7843.625*	7.437			7860.538‡	7.449			8131.702†	7.442	7.950	8.103
7843.628*	7.438			7862.527‡	7.540			8131.705†	7.443	7.960	8.110
7843.629*	7.436	7.945	8.093	7870.517‡	7.417			8131.708†	7.450	7.957	8.112
7843.631*	7.439			7898.656*	7.516	8.063	8.278	8131.712†	7.439	7.958	8.116
7843.632*	7.438	7.947	8.107	7898.658*	7.515	8.058	8.246	8163.667†	7.417	7.931	8.090
7843.634*	7.437	7.942	8.121	7898.660*	7.509	8.050	8.254	8163.672†	7.420	7.935	8.098
7844.687*	7.492			7900.623*	7.429	7.927	8.063	8163.675†	7.420	7.934	8.095
7844.689*	7.491			7900.625*	7.418	7.912	8.084	8167.693†	7.422	7.951	8.100
7844.689*	7.492	8.012	8.205	7900.627*	7.437	7.915	8.071	8167.697†	7.419	7.947	8.107
7844.691*	7.500			7902.645*	7.424	7.925	8.069	8167.701†	7.425	7.947	8.110
7844.692*	7.490	8.015	8.210	7902.646*	7.426	7.926	8.087	8168.665†	7.433	7.951	8.115
7844.694*	7.499	8.030	8.203	7902.648*	7.436	7.939	8.056	8168.669†	7.427	7.950	8.118
7845.648*	7.424			7903.642*	7.420	7.916	8.086	8168.674†	7.429	7.951	8.116
7845.651*	7.411			7903.645*	7.428	7.915	8.088	8168.677†	7.444	7.961	8.123
7845.651*	7.422	7.924	8.083	7903.646*	7.424	7.914	8.067	8169.671†	7.420	7.931	8.101
7845.653*	7.424			7912.659*	7.413	7.919	8.070	8169.676†	7.419	7.926	8.100
7845.653*	7.410	7.913	8.098	7912.664*	7.431	7.923	8.025	8169.679†	7.413	7.934	8.094
7845.683*	7.423	7.921	8.073	7912.666*	7.434	7.912	8.090	8175.685†	7.448	7.964	8.134
7847.648*	7.481			7913.632*	7.437	7.918	8.088	8175.689†	7.455	7.969	8.135
7847.651*	7.487			7913.646*	7.410	7.922	8.081	8175.692†	7.446	7.964	8.135
7847.651*	7.480	8.015	8.204	7913.638*	7.425	7.906	8.083	8182.598†	7.456	7.972	8.116
7847.653*	7.498			7915.644*	7.420	7.917	8.067	8182.602†	7.449	7.966	8.126
7847.653*	7.486	8.014	8.197	7915.646*	7.429	7.925	8.089	8182.605†	7.452	7.966	8.124
7847.656*	7.497	8.033	8.220	7915.648*	7.424	7.915	8.095	8185.624†	7.444	7.938	8.115
7848.563‡	7.429			8093.780†	7.435	7.956	8.102	8185.627†	7.442	7.949	8.110
7849.628*	7.422			8093.784†	7.438	7.960	8.094	8185.630†	7.443	7.958	8.109
7849.630*	7.428										

Observers: §The late J. Ells; *The late R. E. Fried; †J. Lines; ‡D. Pray.

exceptional, and its primary star is a main-sequence object. There are several composite-spectrum systems known to have double secondaries (e.g. d Ser, HR 2024, HR 6497, HR 7508), but the periods of their outer orbits are all more than a year.

A short period and a large mass function (implying a high orbital inclination) normally betoken a relatively good prospect of eclipses. We had already obtained RV traces close to times of the relevant conjunctions without seeing evidence of eclipses in the form of a radical increase in the depth of the dip, but in 1989 photoelectric photometry was requested privately from several amateur observers. The objective was not only to look for eclipses at the known times of conjunction but also to see whether there were other systematic phase-related changes arising from ellipticity or RS CVn-type activity of the primary star.

We were fortunate to receive photometry from R. E. Fried, D. Pray, J. Lines and P. Ells – the last-named wrote on behalf of his father, Mr J. W. Ells, who had observed our star despite the onset of terminal illness. All observers used HD 216380 and HD 214165 as the comparison and check stars, respectively, and presented their results as differential V magnitudes. Fried and Pray also provided differential magnitudes in B and U. Their photometry, listed in Table 2, did not show any unambiguous relationship to orbital phase, and it did not reveal any eclipses associated with the 55-d orbit. What it did show was summarized in another unfortunate remark in the Griffin (1990) paper – 'Photometry shows variations that are seemingly capricious over a range of about $0^{\rm m}.1$, but may be compromised by the presence of a companion star 8″ distant.' The possibility of eclipses with a periodicity other than 55 d was regrettably not considered, and in any case the photometric material was not sufficiently abundant to support a search for a much shorter period. The presence of a companion star, at an angular distance comparable with the radii of apertures typically used in conventional photoelectric photometry, and of a brightness such as to make a difference of about 0.1 mag depending upon its inclusion or exclusion by the aperture, did arouse enough misgivings at the time that the evidence, contained in the measurements, for an eclipse of a short-period *secondary* was unfortunately overlooked.

It is no disparagement of the work of the amateur astronomers who so kindly responded to our request if we find (Section 7.6) that their observations (and those made by *Hipparcos*) would not support a fully sophisticated treatment of eclipses that take place on a time-scale a hundred times shorter than those for which they

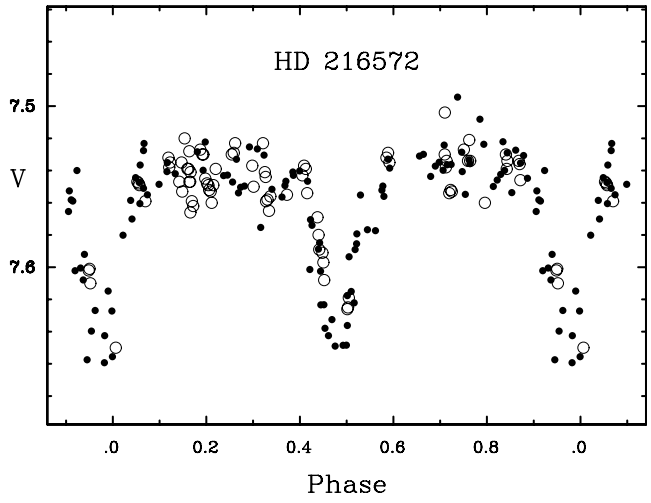

Figure 1. Combined photometry of HD 216572 in the *V* band, observed from the ground (open circles) and by *Hipparcos* and transformed (filled dots), folded about the *Hipparcos* period of 1.184 75 d. The epoch of principal eclipse (T) = JD 244 8501.0739

were invited to search. We apologize to those observers for having failed to appreciate the significance of facts which, taken together and viewed in retrospect, ought to have provided a strong clue as to the true nature of the HD 216572 system.

That nature was disclosed, fully fledged, upon the publication by ESA (1997, vol. 12, p. A515) of the *Hipparcos* results, which showed HD 216572 to be an eclipsing variable with a period of 1.184 75 d; the eclipses appear to be equally spaced and equally deep, indicating two mutually similar stars in a circular orbit. The *Hipparcos* authors had already arranged for HD 216572 to receive the variable-star designation V453 Cep (Kazarovets et al. 1999).

The photometric campaign which we instigated took place in 1989 and 1990, and happened to be contemporaneous with the early part of the *Hipparcos* mission. The ground-based photometry in the *V* band can usefully be plotted on the same graph as the *Hipparcos* photometry by the application of a constant offset in *V*; we used an empirical offset of −0.11 mag, whereas the recipe in the *Hipparcos* Catalogue (ESA 1997, vol. 1, p. 59) would have given −0.127 mag. Strictly speaking the offset ought to change during the eclipses owing to small alterations in the integrated colour of the object, as only the (blue) sub-system is affected: the eclipse depth in *V* could be expected to be slightly less than in H_P for that reason.

In Fig. 1 we plot the transformed *Hipparcos* H_P photometry together with the *V* magnitudes that were kindly supplied by the photometric observers, the time axis being folded on the period already determined by *Hipparcos*. We analyse the eclipse photometry in Section 7.

4 SPECTROSCOPIC OBSERVATIONS

In order to investigate the nature of the individual component stars in HD 216572 we undertook a programme of high-dispersion spectroscopy, employing techniques that enabled us to isolate, classify and measure the spectra of the individual stars.

Two photographic spectrograms of HD 216572 at 8.8 Å mm^{-1} were obtained on baked IIa–O plates with the Calar Alto (CA) 2.2-m telescope in 1987 and 1990; both spectra were widened to 1.5 mm, and have signal-to-noise (S/N) ratios generally in the region 30–50. The plates were processed, intensity-calibrated and reduced in the manner described elsewhere (Griffin 1979). Spectra were extracted in steps of 50 mÅ for λλ3650–4650 Å.

The composite spectrum is strongly hot-dominated in the Ca II H&K region. Subtraction of the primary spectrum using an appropriate surrogate for the giant component (Section 5.1.1) revealed a double K line on both photographic spectra, thus reinforcing the *Hipparcos* announcement. But while the large mass function was thus explained, the determination of the mass ratio of the longer-period system would evidently be complicated by the need to determine the mass ratio of the secondary pair in order to map the velocity changes of its centre of mass. To that end, we recorded, during the course of 5 years, over 80 high-dispersion spectra with a SITe-4 CCD and the 96-inch camera at the coudé focus of the DAO 1.2-m telescope; the spectra are ∼140 Å long, and have a resolving power of some 90 000, a reciprocal dispersion of ∼2.4 Å mm^{-1}, and S/N ratios mostly of the order of 60–120 near λ4481 Å and 30–50 near λ3950 Å. While good S/N ratios were required because the rotational broadening of the secondary lines accentuates difficulties of measurement, exposure times had to be curtailed to avoid excessive smearing brought about by the rapid variations of the secondaries' RVs. We therefore limited exposures to 1 h, or to 2 h if they were centred on a node, and were consequently reliant upon nights of tolerably good seeing. Spectra of appropriate standards were also observed with the same equipment so that they had the same resolution and instrumental profile as did the spectra of the programme star. All observations were reduced with IRAF to one-dimensional spectra; their wavelength scales were those of the rest frame of the primary (HD 216572 A), or the stellar rest frame in the case of a single standard. Table 3 contains a log of our spectroscopic observations of HD 216572 which have contributed to the analysis described in this paper. Those marked with † in columns 8–9 were observed when the secondary sub-system was at a single-lined phase.

We note parenthetically that our spectroscopic observations of HD 216572 did not include any contribution from the faint optical companion because the entrance slit was small enough to exclude it, even though the same is not true for photometric observations (see Section 7).

It had been our intention to divide the observations between the regions of the Ca II K line and of Mg II λ4481 Å; the latter feature is narrower than the K line and should therefore in principle give rise to more precise measurements even though the flux from a hot secondary is less in the blue compared to the violet. However, the early material indicated not only the presence of a substantial interstellar (IS) Ca II line but also a broad and somewhat variable (presumably chromospheric) Ca II emission, strong enough to distort the profiles of the secondary-star K lines. Later observations were therefore confined to the Mg II region, apart from a pair at Hδ intended for investigating stellar temperatures. Observations at phases when the secondary was single-lined were also useful for comparing with standard or synthetic spectra.

In this paper, Section 5 describes the isolation of the spectra of the secondary, HD 216572 B, Section 6 the determination of the mass ratio and individual stellar masses both of the inner pair and of the outer binary, and Section 7 the derivation of an accurate photometric model for the system and the physical parameters of the component stars. Sections 8 and 9 address the evolutionary status of the HD 216572 system and the significance of the chromospheric emission.

Table 3. Log of spectroscopic observations of HD 216572, with orbital phases and computed RVs of the giant component, and including measurements of the RVs of the secondary components.

Observation ID	Date (UT)	MJD	Central λ (Å)	Outer phase	RV giant	Inner phase	RV comp 2	RV comp 3
CA 3620	1987 Nov. 16.769	47115.769	3650–4650*	.739	+13.3	.883	(+115.4)	(−112.4)
CA 4353	1990 Aug. 30.037	48133.037	3650–4605*	.330	+5.9	.536	(−143.4)	(+187.2)
DAO 12238	2000 Sep. 13.315	51800.314	3933	.352	+15.3	.002	(+151.0)	(−192.7)
DAO 15814	2000 Nov. 11.166	51859.166	4481	.427	+43.0	.677	−114.1	+45.0
DAO 15815	2000 Nov. 11.208	51859.208	4481	.428	+43.2	.712	−35.7†	
DAO 15949	2000 Nov. 14.103	51862.103	4481	.481	+55.6	.156	+43.6	−141.3
DAO 16005	2000 Nov. 15.111	51863.111	3933	.499	+58.3	.007	(+154.4)	(−204.7)
DAO 16012	2000 Nov. 15.158	51863.158	4481	.500	+58.4	.047	+121.9	−210.7
DAO 16013	2000 Nov. 15.201	51863.201	4481	.501	+58.5	.083	+102.0	−206.9
DAO 16083	2000 Nov. 16.110	51864.110	4481	.518	+60.1	.850	+48.1	−159.9
DAO 16085	2000 Nov. 16.157	51864.157	3933	.519	+60.1	.890	(+142.4)	(−168.6)
DAO 16086	2000 Nov. 16.199	51864.199	3933	.519	+60.2	.925	(+148.6)	(−198.2)
DAO 16229	2000 Nov. 19.147	51867.147	4481	.573	+59.7	.414	−201.1	+104.5
DAO 16230	2000 Nov. 19.189	51867.189	4481	.574	+59.6	.449	−210.9	+117.1
DAO 16378	2000 Nov. 21.217	51869.217	4481	.611	+54.5	.161	+31.1	−150.4
DAO 16447	2000 Nov. 22.099	51870.099	4481	.627	+51.2	.905	+99.3	−192.1
DAO 16448	2000 Nov. 22.141	51870.141	4481	.628	+51.0	.941	+111.2	−205.1
DAO 16449	2000 Nov. 22.183	51870.183	4481	.629	+50.9	.976	+122.0	−222.6
DAO 16526	2000 Nov. 23.153	51871.153	4481	.646	+46.4	.795	−28.5†	
DAO 16527	2000 Nov. 23.193	51871.193	4481	.647	+46.2	.828	+2.7†	
DAO 11351	2001 Aug. 18.404	52139.404	3933	.549	+60.9	.220	: †	
DAO 18045	2001 Dec. 25.195	52268.195	3933	.903	−57.2	.929	(+161.0)	(−135.0)
DAO 18269	2001 Dec. 30.197	52273.197	3933	.994	−80.4	.151	(+121.6)	(−91.8)
DAO 14267	2002 Aug. 21.436	52507.436	3933	.275	−18.9	.867	(+114.8)	(−136.2)
DAO 14268	2002 Aug. 21.478	52507.478	3933	.276	−18.5	.903	(+140.1)	(−140.5)
DAO 14304	2002 Aug. 22.299	52508.299	4481	.291	−11.7	.596	−145.9	+121.4
DAO 14305	2002 Aug. 22.341	52508.341	4481	.291	−11.4	.631	−119.6	+99.0
DAO 14308	2002 Aug. 22.432	52508.432	3933	.293	−10.6	.708	(−73.1)	(+50.4)
DAO 14309	2002 Aug. 22.475	52508.475	3933	.294	−10.3	.744	: †	
DAO 14310	2002 Aug. 22.513	52508.513	3933	.295	−9.9	.775	: †	
DAO 14359	2002 Aug. 23.415	52509.415	4481	.311	−2.5	.538	−173.6	+147.0
DAO 14360	2002 Aug. 23.456	52509.456	4481	.312	−2.2	.572	−159.2	+137.0
DAO 14412	2002 Aug. 24.352	52510.352	4481	.328	+5.1	.329	−98.4	+57.4
DAO 14413	2002 Aug. 24.394	52510.394	4481	.329	+5.5	.364	−121.5	+87.7
DAO 14463	2002 Aug. 25.345	52511.345	4481	.346	+13.0	.167	+80.0	−103.9
DAO 14464	2002 Aug. 25.387	52511.387	4481	.347	+13.3	.202	−22.0†	
DAO 14465	2002 Aug. 25.435	52511.435	4481	.348	+13.7	.243	−25.0†	
DAO 14698	2002 Aug. 29.301	52515.301	3933	.419	+40.3	.506	(−186.9)	(+158.5)
DAO 14699	2002 Aug. 29.344	52515.344	3933	.419	+40.5	.542	(−178.3)	(+158.7)
DAO 14701	2002 Aug. 29.387	52515.387	4481	.420	+40.8	.579	−187.9	+115.7
DAO 14702	2002 Aug. 29.429	52515.429	4481	.421	+41.0	.614	−156.8	+93.2
DAO 16658	2002 Sep. 18.183	52535.183	4481	.782	−5.9	.288	−26.6†	
DAO 16659	2002 Sep. 18.225	52535.225	4481	.783	−6.3	.323	−79.9	+52.5
DAO 16660	2002 Sep. 18.267	52535.267	4481	.784	−6.6	.359	−122.3	+91.7
DAO 16711	2002 Sep. 19.256	52536.256	4481	.802	−14.9	.194	+10.5†	
DAO 16712	2002 Sep. 19.301	52536.301	4481	.802	−15.2	.232	−2.5†	
DAO 16713	2002 Sep. 19.344	52536.344	4481	.803	−15.6	.268	−15.6†	
DAO 17100	2002 Sep. 25.219	52542.219	4481	.911	−60.0	.227	+15.9†	
DAO 17101	2002 Sep. 25.261	52542.261	4481	.911	−60.2	.262	+10.7†	
DAO 17102	2002 Sep. 25.303	52542.303	4481	.912	−60.5	.298	+34.4†	

*Photographic observation; this column indicates the spectral range.

†Single-lined phase of secondary; individual velocities could not be measured.

: Measurement distorted by IS Ca II K line.

Note: Secondary RVs given in brackets were measured from the K line or on lower-dispersion plates, and were not included in the orbit solution.

Table 3 – *continued*

Observation ID	Date (UT)	MJD	Central λ (Å)	Outer phase	RV giant	Inner phase	RV comp 2	RV comp 3
DAO 17103	2002 Sep. 25.344	52542.344	4481	.913	−60.8	.332	−62.7	+89.7
DAO 17104	2002 Sep. 25.387	52542.387	4481	.914	−61.0	.369	−112.5	+126.9
DAO 17155	2002 Sep. 26.345	52543.345	4481	.931	−66.5	.176	+71.9†	
DAO 18185	2002 Oct. 12.296	52559.296	4481	.223	−41.7	.641	−108.5	+115.5
DAO 18186	2002 Oct. 12.317	52559.317	4481	.223	−41.5	.659	−66.9	+92.2
DAO 18455	2002 Oct. 16.336	52563.336	4481	.297	−9.1	.051	+136.8	−179.5
DAO 13682	2004 Jul. 22.389	53208.389	4481	.085	−81.1	.526	−129.9	+190.4
DAO 13683	2004 Jul. 22.431	53208.431	4481	.086	−81.0	.561	−121.1	+183.1
DAO 13684	2004 Jul. 22.472	53208.472	4481	.087	−80.9	.596	−98.9	+163.1
DAO 13733	2004 Jul. 23.392	53209.392	4481	.104	−78.4	.372	−80.3	+141.0
DAO 13734	2004 Jul. 23.435	53209.435	4481	.104	−78.2	.409	−114.3	+162.5
DAO 13735	2004 Jul. 23.478	53209.478	4481	.105	−78.1	.445	−137.6	+179.3
DAO 13785	2004 Jul. 24.363	53210.363	4481	.121	−74.9	.193	+20.0†	
DAO 13786	2004 Jul. 24.404	53210.404	4481	.122	−74.7	.226	+7.5†	
DAO 13787	2004 Jul. 24.443	53210.443	4481	.123	−74.6	.259	+11.8†	
DAO 13838	2004 Jul. 25.397	53211.397	4481	.140	−70.3	.065	+170.4	−132.5
DAO 13839	2004 Jul. 25.440	53211.440	4481	.141	−70.1	.101	+150.5	−108.9
DAO 13890	2004 Jul. 26.396	53212.396	4481	.159	−65.1	.908	+146.3	−117.8
DAO 13891	2004 Jul. 26.438	53212.438	4481	.159	−64.8	.944	+176.6	−135.7
DAO 19956	2004 Sep. 14.342	53262.342	4481	.071	−82.5	.066	+163.5	−142.0
DAO 20044	2004 Sep. 17.475	53265.475	4481	.129	−73.2	.711	−7.0†	
DAO 20090	2004 Sep. 18.418	53266.418	4481	.146	−68.8	.507	−154.1	+189.3
DAO 20091	2004 Sep. 18.462	53266.462	4481	.147	−68.6	.544	−138.7	+182.9
DAO 20189	2004 Sep. 20.278	53268.278	4481	.180	−58.1	.077	+154.6	−137.1
DAO 20190	2004 Sep. 20.321	53268.321	4481	.181	−57.8	.113	+133.8	−112.3
DAO 20191	2004 Sep. 20.363	53268.363	4481	.181	−57.5	.149	+101.6	−82.3
DAO 25	2005 Jan. 3.117	53373.117	4481	.096	−79.6	.569	−121.3	+173.5
DAO 26	2005 Jan. 3.159	53373.159	4481	.097	−79.5	.605	−92.2	+159.9
DAO 78	2005 Jan. 4.072	53374.072	4481	.113	−76.6	.375	−79.8	+140.7
DAO 79	2005 Jan. 4.115	53374.115	4481	.114	−76.4	.411	−113.8	+153.3
DAO 202	2005 Jan. 6.088	53376.088	4481	.150	−67.6	.077	+161.8	−133.0

†Single-lined phase of secondary; individual velocities could not be measured.

5 THE SPECTRA OF HD 216572 B

5.1 Isolating the spectra

We uncovered the spectrum of the hot secondary component by the technique of digital subtraction (see Griffin 1986).

5.1.1 CA photographic spectra at 8.8 Å mm^{-1}

Our photographic spectra are particularly useful in that they span a region that is broad enough to include a number of temperature- and luminosity-sensitive features. Trial subtractions resulted in our selecting λ Peg, classified as G8 IIIa CN0.5 (Keenan & McNeil 1989), as the surrogate primary, though among the late-G giants in our library of standards 31 Vul and 15 Cyg, classified by the same authors as G7 III Fe-1 and G8 III, respectively, were almost equally good. Because the heavy veiling of the primary's lines by the dominant secondary spectrum results in a relatively small contribution from the former, it was not easy to make an unambiguous choice.

5.1.2 DAO CCD spectra at 2.4 Å mm^{-1}

We subtracted appropriate fractions of a DAO CCD spectrum of λ Peg from each observation (or averaged observation) of the composite spectrum of HD 216572. Figs 2 and 3 illustrate the subtraction procedure near Mg II λ4481 Å and the Ca II K line, respectively, at phases when the secondary spectra were well separated.

5.2 The spectral type of HD 216572 A

Since our standards for G7 III, G8 III and G8 IIIa appeared almost equally good as surrogates for HD 216572 A, we judged the latter to have a spectral type of G8 III.

5.3 The spectral type of HD 216572 B

The two stars comprising the secondary of HD 216572 are clearly very similar. As is characteristic of a late-B dwarf, the combined secondary spectrum shows very few strong lines besides the Balmer lines, the Ca II K line and the Mg II line at λ4481 Å. Unfortunately none is ideal for classifying this pair. Most of the observations corresponded to double-lined phases, and the Balmer lines are merely widened, being too broad to be resolved (see Fig. 3). The strength of the Mg II line is insensitive to changes in $T_{\rm eff}$ in this spectral range (see Section 7.2.2). Some (but not all) spectra of the K-line region show weak, broad emission whose presence interferes significantly with the K-line profile of one or other component of the secondary system.

The spectrum of HD 216572 B matches quite closely that of ν Cap, though there is a tendency for lines in the latter to be

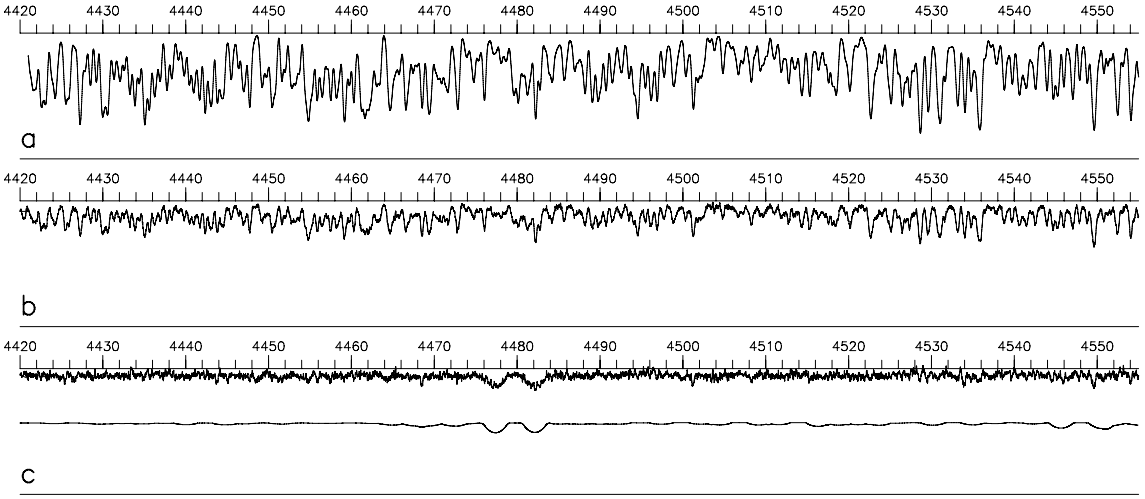

Figure 2. Isolation of the spectrum of HD 216572 B in the vicinity of the Mg II doublet at λ4481 Å, from CCD observations. The surrogate primary, λ Peg, panel (a), used to subtract the spectrum of the cool giant from the composite spectrum, shown in panel (b), needed to be blurred by 15 km s^{-1} to mimic the rotational broadening of the lines in the cool primary. The upper tracing in panel (c) is the uncovered spectrum of the double-lined secondary; the lower one is a composite of two identical ∼ B9 V spectra, computed for $T_{\rm eff} = 10\,300$ K, $\log g = 4.0$ (Vrancken, unpublished thesis), mutually displaced by 316 km s^{-1} and blurred by a rotational velocity of 95 km s^{-1}.

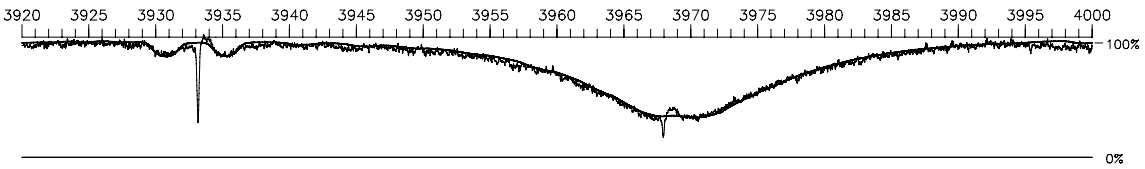

Figure 3. The spectrum of HD 216572 B in the region of the Ca II H&K lines at λλ3968 and 3933 Å, observed when the two K lines were widely separated. The profile with the slight noise (and the sharp IS lines) is that of HD 216572 B after subtraction of the contribution of HD 216572 A from the observed spectrum, as in Fig. 2; the smooth profile is a synthetic spectrum. The broad absorption feature near the Ca II H line is Hϵ. The distortion just redward of the interstellar lines is ascribed to chromospheric emission in HD 216572 A.

slightly stronger than in HD 216572 B. Gray & Garrison (1987)'s classification of ν Cap as B9.5 V is well supported by values of $T_{\rm eff} = 10\,250 \pm 100$ K calculated by Adelman et al. (2002) and $M_V = +0.14$ derived via the *Hipparcos* parallax.

Comparisons between a single-lined secondary spectrum and a suite of synthetic spectra for B-type stars, described by Vrancken et al. (1997) and kindly made available by M. David (private communication), indicated a best fit with parameters $T_{\rm eff} = 10\,300 \pm 200$ K, $\log g = 4.0$, the uncertainty in $T_{\rm eff}$ being estimated from fitting to the Balmer line. The model includes a microturbulence of 2.0 km s^{-1}. According to Schmidt-Kaler (1982) a dwarf with that temperature has a spectral type close to B9. We have therefore adopted B9 V as the combined spectral type of the secondary stars.

In Fig. 3 the spectrum of HD 216572 B is compared with a composite model constructed from two identical Vrancken models, each for $T_{\rm eff} = 10\,300$ K, $\log g = 4.0$ and blurred by 95 km s^{-1} to mimic the observed stellar linewidths, and separated in RV by the measured mutual displacement. The amount of blurring was judged by eye; it was difficult to define it precisely for lines that are so wide, and is uncertain by at least 10 km s^{-1}. As will be described in Section 7.2.2, the components appear to differ slightly in luminosity, so the synthetic spectra were averaged in the ratio of 1:1.07 to emulate the luminosity ratio given in Table 7.

6 MASS RATIO OF THE HD 216572 SYSTEM

The mass ratio, q, of the components of a binary star can be measured simply and directly from the inverse of their velocity ratio: $q = M_1/M_2 = -v_2/v_1$, where v is the velocity relative to the γ-velocity and subscripts 1 and 2 refer to the primary and secondary, respectively. The fact that the secondary of HD 216572 is itself a double star clearly presents an added complication, since it is necessary to determine the orbit of the secondary sub-system and to track its γ-velocity displacements in relation to the velocity of HD 216572 A. That complication is handled by a triple-line modification of our spectroscopic-binary orbit code.

6.1 RV measurements of the secondary stars

The positions of the features in the two secondary stars were measured by cross-correlation. In the combined secondary spectra the Balmer lines are not even partly resolved at any phase owing to their large intrinsic widths, and were therefore eliminated from the cross-correlation. Of the remaining features only the Ca II K line and the Mg II line at λ4481 Å are sufficiently prominent for measurement, so to avoid diluting the signal with noise from non-contributing regions of the continuum we limited the cross-correlation windows to a 30-Å region centred at λ3935 and a 40-Å one centred at λ4485 Å. Since the lines of the good stellar match (ν Cap) are slightly broader

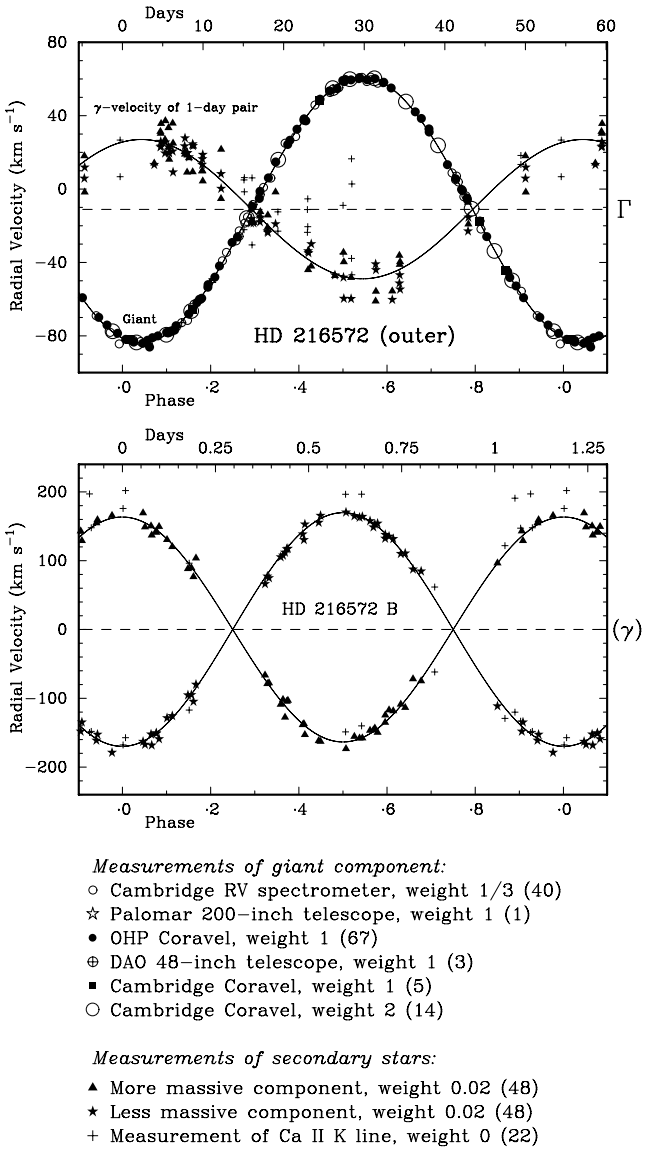

Figure 4. Upper panel: the outer orbit of HD 216572. Lower panel: the secondary orbit based on velocities measured from the Mg II line. A key to sources of observations, including weights (and numbers), is also indicated.

than those of HD 216572 B we used as the template for the cross-correlations the Vrancken model for $T_{\rm eff} = 10\,300$ K, $\log g = 4.0$, appropriately broadened.

The presence of a substantial IS K line interfered with the cross-correlations at that wavelength, while the additional presence of Ca II emission, presumably arising in the chromosphere of the giant, also caused distortion in some of the spectra (see Fig. 3). Results from the K-line region were therefore not used in this analysis; they are given in brackets in Table 3, and are represented by plusses in Fig. 4.

6.2 Orbital solutions

Since the secondary spectra had been extracted in the rest frame of the primary star, the displacements which we measured were with respect to that reference frame. We therefore corrected them for the absolute velocities of the cool-giant primary as given for the relevant dates of observations by the single-lined orbit. The sets of velocities for all three stars were then solved simultaneously by a triple-line version of the orbit-solving software (Griffin 2001) which is used routinely in this work. A non-zero eccentricity can often be maintained for the inner orbit of a triple system by perturbations caused by the singleton in the outer orbit (Mazeh 1990), but in this case the inner orbit is not distinguishable from a circle. The solution therefore employed simultaneously a Lehmann-Filhés (1894) solution for the outer orbit and a Sterne (1941) one for the inner, and adopted weights of 0.02 for the velocities of each of the B stars in the inner orbit in order to equalize the variances of the observations of the three stars. Since the B-star velocities therefore jointly constitute only about 1.6 per cent of the weight of the whole data set, the solution for the outer orbit is very similar to that for the giant component alone. Any circularity of argument that may be implied by the use of the single-lined orbit in deducing the velocities of the B stars for entry into the full solution is therefore not a matter for concern. The elements now derived for the late-type primary star are very similar to those given previously (Griffin 1990), but with improved standard deviations – by a factor of 16 in the case of the period. Our final orbital elements are given in Table 4 for the outer system and Table 5 for the inner one. The two orbits are illustrated in Fig. 4.

The period given for the inner orbit in Table 5 on the basis of our spectroscopic observations has a standard deviation of ∼0.25 s. It can be refined further by appeal to the epoch of eclipse (JD = 244 8501.0739), given in the *Hipparcos* catalogue (vol. 11, p. P26, where the object is identified as no. 112972). That

Table 4. Orbital elements for HD 216572 (A + B).*

P	=	54.7176 ± 0.0003 d
$(T)_{42}$	=	MJD 48990.4 ± 3.7
Γ	=	-11.10 ± 0.09 km s^{-1}
K_1	=	72.35 ± 0.12 km s^{-1}
K_2	=	38.0 ± 0.9 km s^{-1}
q	=	0.525 ± 0.013
e	=	0.0042 ± 0.0017
ω	=	$164\overset{\circ}{.}3 \pm 24\overset{\circ}{.}6$
$a_1 \sin i_{\rm o}$	=	54.44 ± 0.09 Gm
$a_2 \sin i_{\rm o}$	=	28.6 ± 0.7 Gm
$M_{\rm G} \sin^3 i_{\rm o}$	=	2.62 ± 0.08 M$_\odot$
$M_{\rm 2B} \sin^3 i_{\rm o}$	=	5.00 ± 0.09 M$_\odot$

*2B denotes the combined inner system.

Table 5. Orbital elements for HD 216572 B.*

P	=	1.184 725† ± 0.000 003 d
T_0	=	MJD 52679.3784 ± 0.0013
K_1	=	163.4 ± 1.3 km s^{-1}
K_2	=	169.8 ± 1.3 km s^{-1}
q	=	1.039 ± 0.011
e	≡	0
ω is undefined in a circular orbit		
$a_1 \sin i_{\rm i}$	=	2.662 ± 0.020 Gm
$a_2 \sin i_{\rm i}$	=	2.766 ± 0.020 Gm
$M_{\rm B1} \sin^3 i_{\rm i}$	=	2.319 ± 0.030 M$_\odot$
$M_{\rm B2} \sin^3 i_{\rm i}$	=	2.232 ± 0.029 M$_\odot$

*The component stars are denoted by B1 and B2.
†This value is slightly refined to 1.184 7205 (see Section 6.2).

epoch – corresponding to phase .75 in the spectroscopic convention adopted here – is found to be close to $3529^1/_4$ periods before the T_0 in Table 5. Dividing the interval between the *Hipparcos* and spectroscopic epochs by that number exactly, we obtain the period as 1.184 7205 d. The uncertainties in *Hipparcos* epochs are indicated in the catalogue only to an order of magnitude, which in the relevant case is 0.001 d. If we took the quadratic sum of the uncertainties of our own and the *Hipparcos* epochs, which are separated by more than 4000 d, as being 0.002 d, that would correspond to an uncertainty in the period of 0.05 s. At such a level of precision, it is necessary to distinguish between the true period (in the rest frame of the system) and the observed period, which is slightly shortened in this case by the modest velocity of approach (the Γ-velocity) of the system. The true period is 1.184 765 d, which differs by about 70 standard deviations from the observed one.

The masses of the two B9 dwarfs differ slightly, by 4 ± 2 per cent according to Table 5. It will also be shown (Section 7.6) that $\sin^3 i_i$ is close to 0.9, and that the actual masses are near 2.6 and 2.5 $M_\odot$ and thus lie very close to the mean relationship published by Andersen (1991) for stellar mass versus $(B - V)$. The value of 2.7 $M_\odot$ derived in Section 7.6 for the mass of the G8 component is also unexceptional.

7 PHOTOMETRIC AND PHYSICAL PARAMETERS OF THE COMPONENTS

Important information about the luminosities of the components in a binary system and about the system's reddening can be gained by modelling the observed photometry. For HD 216572 the photometry of the partially eclipsing inner system provides an independent assessment of the radii of the hot pair, and of the geometry of both orbits.

The construction of a full photometric model for HD 216572 involved three distinct steps: first, removing the contribution from the faint visual companion (at an angular distance of only 8 arcsec, it will have been included in all the photometry which is utilized in this paper); secondly, apportioning the combined photometry between the hot and the cool components by treating the secondary as a single star; and lastly, removing the contribution of the spectroscopic primary (HD 216572 A) and modelling the eclipse as depicted by the residual magnitudes. Step two also yields the colours of the secondary system. Step three yields the radii and luminosities of both B-type components and the minimum separation between their centres, projected on to the plane of the sky. In practice the steps were iterative rather than sequential.

7.1 The outer system

The published photometry for HD 216572, detailed in Section 1, is slightly discordant. Moreover, while Blanco et al. (1955) do not give the dates of their photometry, they comment that they averaged observations made on two or three nights, so it is statistically likely that one or more of their measurements corresponded to a partial-eclipse phase of the secondary. A similar bias must also affect the *Hipparcos* measurements, 35 per cent of which were made during eclipses. The published photometry of HD 216572 may therefore be more uncertain than was thought, and redder by ∼0.02 mag on average than it ought to be. Fortunately we also have at our disposal the unpublished photometry from the amateur group (see Section 3), collectively representing 100 data points in V and 74 each in B and U. By referring specifically to non-eclipse phases we derive $V = 7.43$ mag, $B = 7.94$ mag, $U = 8.09$ mag, i.e. $B - V = 0.51$ mag, $U - B = 0.15$ mag.

7.1.1 Correcting for the visual secondary

We deduced in Section 1 that the visual secondary contributes some 9 per cent to all the observed photometric intensities, so that amount was subtracted from each one. We used the same percentage for each wavelength band, implicitly assuming that the two visual components are of similar colours. An attempt to measure the velocity of the visual secondary with the RV spectrometer gave no result, which is generally an indication that the star is of early type. Although its $(B - V)$ colour index was measured by *Tycho* as 0.97 mag, much redder than the primary, serious discordance (as much as 0.6 mag in V) between the *Tycho* and *Hipparcos* measurements (see Section 1) demonstrates great uncertainty. Even if the visual secondary is in fact somewhat redder than the primary, it is so much fainter that no significant error is introduced by our assuming the visual pair to have the same relative brightness in all colours.

7.1.2 Determining ΔV

ΔV, the difference in magnitude between the primary and the combined secondary, is measured by the subtraction process, in wavelength bands that are compatible with the photometry published by Willstrop (1965) for standard stars. The latter's measurements are normalized in V, so by comparing our fluxes with those for appropriate pairs of standard stars we derive a brightness ratio. For HD 216572 we thus obtained $\Delta V = -0.10 \pm 0.04$ mag, implying that the combined secondary is brighter than the cool giant. It is so, in fact, at all the wavelengths for which we have data. Even in the mid-blue the primary's spectrum is strongly veiled (see Fig. 2); the HD classification for HD 216572 was actually A0. The quoted uncertainty allows for the possibility of bias due to the smallness of the sample of appropriate standards.

7.1.3 Colour indices of the late-type giant

In our analyses of composite spectra we have routinely adopted for the primary component the photometric indices of the surrogate primary, which in this case is λ Peg. However, since λ Peg is itself somewhat reddened we adopted instead the colour indices published for 15 Cyg.

7.1.4 Colour indices of the combined B9 dwarf

We assigned colours to the combined secondary by interpolation in the relevant tables of Schmidt-Kaler (1982, section 4.1) for a dwarf with $T_{\rm eff} = 10\,300$ K.

7.2 The inner system

We recovered the undiluted photometry for the combined secondary, in each wavelength band, by subtracting the photometric intensities corresponding to the (reddened) magnitudes of HD 216572 A – here we are anticipating a result from Table 6 – from each of the observations listed by *Hipparcos* and in Table 2, after correction for the visual secondary star. The mean unreddened colours for the combined secondary were also thereby determined.

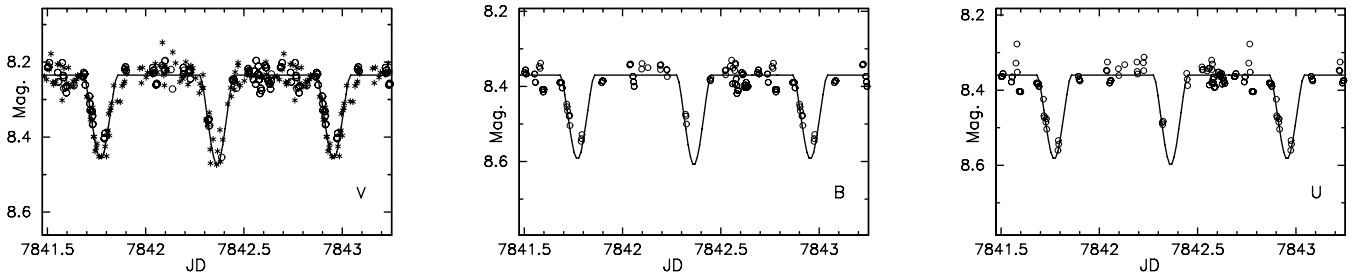

Figure 5. Observed eclipse light curves for HD 216572 B, after the contributions of the late-type giant have been subtracted. Circles represent ground-based photometry, and asterisks (in *V* only) the *Hipparcos* data. The central dip corresponds to the eclipse that occurs when the slightly more massive star is in front. We show more than a complete cycle for the sake of continuity.

7.2.1 Eclipses of the inner system

The eclipse photometry is reproduced in Fig. 5. The ground-based observations are represented by open circles; the asterisks in the *V* plot are the *Hipparcos* observations, which we incorporated after adjusting the published H_P magnitudes by -0.11 mag to align them with the ground-based (V) photometry outside eclipse (see Section 3). The observations were folded about the calculated period and normalized to JD 244 7841.8662 (the first mid-eclipse represented by the photometry).

To analyse the eclipse photometry we adopted a simple model whose adjustable parameters are the radii of the two B stars (and their corresponding values of $\log L$ and M_V), and the minimum projected distance D between their centres. Other parameters that are notionally adjustable are the nett translational velocity of one B star past the other (thereby incorporating i_i, the inclination of the inner orbit) and the mass ratio, q, and its uncertainty; see Table 5. Despite the small distance of only 4.1 $R_\odot$ (if $i_i = 75^\circ$; see below) between the stellar surfaces, the light curves do not appear to be noticeably affected by ellipticity or reflection effects, though those could be somewhat disguised by the noise; we placed an upper limit of 0.02 mag on such curvature, and neither effect was included in our model. Limb darkening was calculated from the 'square-root' law, coefficients being interpolated from van Hamme (1993).

Fig. 5 gives the impression that the central dip (or 'primary eclipse') is slightly (<0.02 mag) deeper than the secondary dip. It is the one when the more massive star (which we identify as the primary) is in front. Since the orbit is circular the geometry of the two eclipses is identical, so exactly the same area of stellar surface is hidden at either eclipse. The primary star must therefore be the one with the lower surface brightness, so it is either a little cooler than the secondary, or a little larger, or both. According to stellar-evolution theory both possibilities are consonant with the primary being slightly the more massive of a coæval pair, so it is likely that both effects are present.

7.2.2 The temperatures of the B stars

Lack of obvious spectral-line indicators strongly suggests that ΔT ($=T_1-T_2$) is small, and since the associated uncertainty may exceed the quantity itself it needs independent methods of measurement to be certain of its sign. Section 5.3 found $T = 10\,300 \pm 200$ K for the combined secondary by matching to a synthetic spectrum, though we now raise the uncertainty to ± 500 K to include uncertainties in the model as well. We can measure ΔT via the equivalent widths (EW) of the Ca II K line and the Mg II λ4481 Å line. At double-lined phases both appear weakened in the inverse ratio of the component-star fluxes, but the two features actually behave quite differently as T changes. Only the K line is T-sensitive in this range of spectral types, increasing by 75 per cent as T falls from 10 500 to 10 000 K (EW = 410 to 725 mÅ), while the Mg II line (EW = 350 mÅ) barely changes, so a study of the two features can yield both the flux ratio and the temperatures of the two B stars. Equivalent widths were therefore measured on all suitable spectra: nine at the K line and 48 at the Mg II line.

An unweighted average of the EWs of the stellar K lines yielded a difference of only 3.6 per cent between the two stars: 259 ± 24 and 244 ± 14 mÅ for the primary and secondary, respectively. However, the chromospheric emission visible in Fig. 3 will have influenced those EW measurements. The emission appears to vary and is somewhat redshifted, and seven of the nine K-line spectra were observed at phases when the emission is likely to have interfered with (reduced) the EW of the primary B star by an undetermined amount. In one particular pair of sequential observations the primary's K line is quite noticeably smaller than that of the secondary, and if those two measurements of the primary's EW are zero-weighted, ΔEW is four times greater.

On the other hand, the means of the measured strengths of the Mg II line revealed ΔEW of 7.5 per cent (196 ± 4 mÅ for the primary, 181 ± 3 mÅ for the secondary). That therefore represents just the difference in magnitude, the ratio of 1.08 indicating that the primary is 0.08 mag brighter than the secondary. Applying that flux difference to the K-line EWs (and zero-weighting the pair with obvious emission contamination) we obtain 553 ± 38 mÅ for the primary and 507 ± 29 mÅ for the secondary – and incidentally confirming that T is close to 10 300 K for both B stars (as deduced in Section 5.3). We therefore adopted $\Delta T = -100$ K since the small inequality in mass suggests $\Delta T \neq 0$. The measured mean value of 377 mÅ for the combined Mg line also indicates that the Mg abundances in the two stars are not substantially different from the solar values incorporated into the synthetic spectra.

To examine the possibility of systematic errors in the EW measurements such as could arise from a localized preponderance of residual-spectrum mismatch features when the G8 spectrum was subtracted, we treated the 29 Mg-line spectra which had a blueshifted primary separately from the 19 spectra observed at the opposite phases, but the result was inconclusive. Situations that could lead to *apparent* discrepancies, e.g. when one B star was slightly eclipsed, were not investigated since there were not enough spectra of the necessary high quality at all the phases in question.

Trials with $\Delta T = -100$ K yielded $R_{B1} = 2.1$ $R_\odot$, $R_{B2} = 2.0$ $R_\odot$, $\Delta M_{bol} = -0.06$, $D = 2.11 \pm 0.02$ $R_\odot$ as a best fit to the observed photometry; that model is the source of the smooth curve fitted to the data points in Fig. 5. A model with $R_{B1} = 2.2$ $R_\odot$, $R_{B2} = 2.0$ $R_\odot$,

$D = 2.175$ R$_\odot$ gave an equally good visual fit to the photometry but implied a greater disparity in fluxes than the measured EWs indicate. On the other hand, the 4 per cent difference in mass between the two stars given by the orbit solution (Table 5) corresponds to $\Delta M_{\rm bol} > 0.06$ mag. However, the differences in question are all rather small, and can be easily accommodated within the formal uncertainties in the EWs, the adopted stellar parameters and the masses. We therefore conclude that the B-star parameters (which are set out in full in Table 7) are consistent with both the spectroscopic and the photometric observations to well within the uncertainties quoted there.

7.3 Modelling the system's photometry

Values of M_V for the individual B stars and for the combined inner system were calculated from their $T_{\rm eff}$ values and radii, as determined above. M_V for the cool giant was next derived, via ΔV. We could then construct the photometric model given in Table 6, model (i).

A discrepancy of 0.2 mag in $(B - V)$ is revealed between model (i) and observation, but since the strength of the IS K line led us to anticipate quite considerable reddening we have little hesitation in attributing the entire discrepancy to a colour excess of $E(B - V) = 0.20$ mag. The equivalent ultraviolet (UV) excess, $E(U - B) = 0.15$ mag, matches exactly the corresponding discrepancy in $(U - B)$. The conventional extinction ratio $A_V/E(B - V) = 0.31$ led to an overall absorption of $A_V = 0.62$ mag, and we could thence derive the reddened magnitudes of the outer system, given in model (ii), for direct comparison with observation.

While there is evidently a considerable amount of IS Ca II between the Earth and HD 216572, whose Galactic latitude is only 1°.3, there is conflicting evidence as to how much general extinction there may be either towards or embedding the object. On the one hand, Benedict et al. (2002) derived an extinction $A_V = 0.23 \pm 0.03$ mag for δ Cep, which is about 4° away from HD 216572 and slightly more distant (its *Hipparcos* parallax is 0.00332 ± 0.00058 arcsec). On the other hand, the strength of the IS K line in HD 216572 is some 50 per cent greater than in HR 1129 (Griffin, Griffin & Stickland 2006). The distance to HR 1129 (derived from the *Hipparcos* parallax) is only about 5 per cent smaller than to HD 216572, yet Griffin et al. (2006) found $E(B - V) = 0.30$ mag, $A_V = 0.93$ mag. One possibility is therefore the presence of more IS or circumbinary extinction in HD 216572 than the colour excess alone suggests. The strength of selective IS absorption, such as in the K line, does not correlate well with overall light diminution, and we believe that the amount of *reddening* (though not necessarily of *extinction*) incorporated into model (ii) is likely to be broadly correct as it stands.

The accretion column suggested in Section 7.7 below, while indicating the presence of inter-binary material, seems unlikely to be a significant contributor to the overall extinction of the system since its proposed obscuration of the hot inner pair is only about 0.05 mag.

7.4 Luminosities of the component stars

From $R_{\rm B1} = 2.1$ R$_\odot$, $R_{\rm B2} = 2.0$ R$_\odot$, $T_{\rm B1} = 10\,300$ K and $T_{\rm B2} = 10\,400$ K, we calculated $M_{\rm bol}$, interpolating the bolometric corrections (BCs) from table 3 of Flower (1996). From those we derived $M_V = +0.93 \pm 0.22$ mag for B1 and $+1.01 \pm 0.23$ mag for B2, and a combined M_V for the inner system of $+0.22 \pm 0.23$ mag. The uncertainties in the individual values of M_V are quadratic combinations of those in BC (via $T_{\rm eff}$) and in R. The corresponding values of $\log L_{\rm B1}$ and $\log L_{\rm B2}$ are 1.65 ± 0.09 and 1.62 ± 0.10; again, the formal uncertainties were derived by adding quadratically the independent uncertainties in R and in $T_{\rm eff}$ (and thence in BC). Those values of M_V are consonant with ones determined for nearby late-B dwarfs, though the latter reveal a substantial scatter.

Given the constraint of $M_V = +0.22$ mag for the combined dwarf, and since ΔV for the outer system is -0.1 mag, then M_V for the cool giant is $+0.32 \pm 0.27$ mag. That result places the giant star within the range of M_V shown for G8 III stars by Keenan & Barnbaum (1999, their fig. 1), and is close to the value of $+0.23$ mag calculated for 15 Cyg from its tabulated parallax. The system's unreddened M_V is therefore -0.48 ± 0.35 mag. An extinction of $A_V = 0.62$ mag, as deduced above, would give an apparent M_V of $+0.14$ mag for model (ii) in Table 6.

The observed m_V for the complete system is 7.43 mag, of which 7.53 mag represents the triple system of interest here. Since the distance modulus based on the published *Hipparcos* parallax of 0.00389 ± 0.00098 arcsec is 7.05 ± 0.58 mag, the *observed* M_V for the system is $+0.48 \pm 0.58$ mag; that uncertainty fully accommodates the reddened model's value of +0.14 mag. We therefore find model (i) of Table 6 to be a fully satisfactory and internally consistent description of the outer binary system of HD 216572, though the value of A_V deduced from the colour excess alone may only be a lower limit.

7.5 Physical parameters of the cool giant

The physical parameters M, R, $T_{\rm eff}$ and L for all components are needed to compare the positions of the stars in the Hertzsprung–Russell (HR) diagram with stellar-evolution models. For the two B stars those quantities have already been derived, and are given in Table 7. For the G8 III star we first determined $T_{\rm eff}$, and to that end we examined what has been published for the surrogate, λ Peg. Mozurkewich et al. (2003) measured $T_{\rm eff} = 4699 \pm 71$ K from flux integrations, while Smith (1998) determined the slightly higher value of 4800 ± 50 K by line-profile synthesis. We therefore adopted $T_{\rm eff} = 4750$ K for HD 216572 A, with an estimated uncertainty of ± 200 K to allow for the possibility of an inexact match with the surrogate. With $M_V = +0.32$ (Table 6) and a BC interpolated from Flower (1996) we derived $M_{\rm bol} = -0.11 \pm 0.27$, $R_{\rm G} = 14.9 \pm 2.0$ R$_\odot$ and $\log L_{\rm G} = 2.00 \pm 0.07$ (see Table 7). The formal errors are quadratic combinations of the independent uncertainties in $T_{\rm eff}$ and M_V.

7.6 Orbital inclinations and stellar masses

We have seen that, in order to model the inner-system eclipse photometry, we needed to specify an 'impact parameter' of 2.11 R$_\odot$, or 1.47 Gm. The separation of the twin B stars in the 1.18-d subsystem, perpendicular to the line of sight, is also given by $a \cos i_{\rm i} = (a_1 + a_2) \cos i_{\rm i} = 5.43 \cos i_{\rm i}$ Gm (Table 5), so $\cot i_{\rm i} = 1.47/5.43$, or $i_{\rm i} = 74°.8$; its uncertainty, derived from those in a_1, a_2 and D, is of the order of 1° (1.3 per cent in $\sin^3 i_{\rm i}$). We thence calculate individual B-star masses of 2.58 and 2.48 M$_\odot$, deriving uncertainties of ± 0.05 by combining quadratically those given in Table 5 with that given here in $i_{\rm i}$. The sub-system as a whole therefore has a mass of 5.06 ± 0.08 M$_\odot$; the uncertainty now includes (quadratically) that in $i_{\rm i}$.

In the outer orbit (Table 4) the mass of the sub-system is given as $(5.00 \pm 0.087)/\sin^3 i_{\rm o}$ M$_\odot$. Equating that with our value of 5.06 ± 0.08 M$_\odot$ gives $\sin^3 i_{\rm o} = 0.988 \pm 0.023$, leading to $81° \leq i_{\rm o} \leq 90°$. Actually, if the inclination of the outer orbit is greater than 81°.5, eclipses would occur in the 55-d outer orbit, and those have not

Table 6. Photometric model for HD 216572.

Object	M_V	$(B-V)$	$(U-B)$
(i) Unreddened model:			
HD 216572 A (G8 III)	+0.32	0.95	0.69
Combined secondary (B9 V)	+0.22	−0.06	−0.17
System	−0.48	0.31	0.00
(ii) Reddened model:			
HD 216572 A (G8 III)	+0.94	1.15	0.87
Combined secondary (B9 V)	+0.84	0.14	−0.02
System	+0.14	0.51	0.15
Observations:			
HD 216572 (triple system)	+0.48† ±0.58	0.51	0.15

†Based on the *Hipparcos* distance modulus of 7.05 mag.

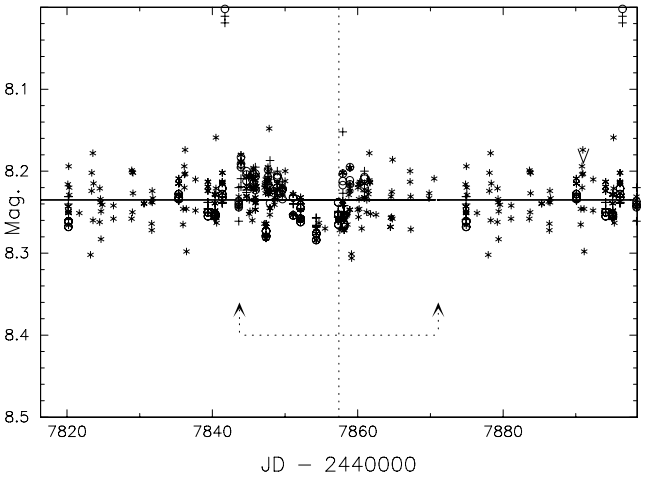

Figure 6. Superimposed photometry of the B stars after the effects of the inner eclipses have been removed. The observations have been wrapped about JD 244 7857.4, with $P = 54.7176$ d. *V* magnitudes are shown by stars, *B* magnitudes by circles, and *U* magnitudes by plusses. The vertical dotted line indicates the date of mid-conjunction; the arrows show the timings of quadrature.

definitely been observed. Use of the above value of $\sin^3 i_o$ enables the mass of the G giant to be determined as 2.65 $M_\odot$. We cannot usefully comment on the likelihood that the inner and outer orbits are coplanar because we have no information on the directions in which they are inclined.

Since the simplicity of our photometric modelling could have introduced systematic errors into our assessment of the B-star parameters, it will scarcely be profitable to pursue a more elegant analysis until more systematic and precise photometry has been obtained. Nevertheless, although the photometric observations did not find evidence of eclipses of the inner pair by the cool giant, it is worth pointing out that small photometric changes which would result from a grazing eclipse could have been confused by the real (though much more rapid) variations arising from the inner-system eclipses. We therefore re-examined the available photometry.

7.7 Possible evidence of mass exchange

Each photometric point plotted in Fig. 5 was corrected for the theoretical dimming due to the secondary eclipses, and re-plotted by folding about the 54.7176-d period of the outer orbit and normalizing to the epoch of conjuction (giant in front), JD = 244 7857.4. The resulting photometry (Fig. 6) does in fact appear to show a small drop in brightness near the centre. However, that 'dip' cannot represent an eclipse of the secondary system by the primary, for three reasons. (a) Its timing precedes that of conjunction (shown by the vertical dotted line in Fig. 6) by some 2–3 d, which is far outside the limits of the uncertainty in the orbit. (b) The 'dip' depth is the same in all three colours, whereas an eclipse of the hot secondaries by the cool giant would be colour-dependent, being most pronounced by far in *U*. (c) Since the apparent light loss is less than 0.05 mag (∼5 per cent), any eclipse would be very shallow and therefore short; instead, the 'dip' is 5–6 d wide. We therefore confirm the upper limit, given above, of 81°.5 for the inclination of the outer orbit.

Those characteristics of the 'dip' feature, together with the hint of a comparably broad feature of similar magnitude but inverted profile centred shortly after the quadrature preceding conjunction (the left arrow in Fig. 6), are reminiscent of the light curves often seen in cataclysmic variables in quiescence. In those cases, they are confidently ascribed to the visibility and then the eclipse of a hotspot where an accretion stream impinges on a disc. It seems doubtful whether the same explanation could serve in the case of HD 216572, since the primary star is at present far from filling its Roche lobe. Any material now being accreted by the secondary sub-system could therefore come only from the primary's stellar wind; moreover, the mechanism of accretion on to a rapidly orbiting double star raises novel uncertainties.

It is not possible to tell whether a small, sharp dip is present or not at the exact date of conjunction. The noise level is sufficient to disguise such a delicate feature, and in any case it would (if present) be confused with the broader dip that precedes it. We may note that the rapid motion of the secondary stars in their own small orbit, which may not be co-planar with the outer one, implies that the exact timing and light curve of any eclipse cannot be specified, and

Table 7. Physical parameters of the components of HD 216572.

Star	Type	M_V (m)	$T_{\rm eff}$ (K)	BC (m)	$M_{\rm bol}$ (m)	R ($R_\odot$)	$\log L$ ($L_\odot$)	M ($M_\odot$)
Giant in outer system:								
HD 216572 A	G8 III	+0.32 ±0.27	4750 ±200	−0.44 ±0.09	−0.11 ±0.27	14.9 ±2.0	2.00 ±0.07	2.65 ±0.08
Inner system:								
Primary	B9 V	+0.93 ±0.22	10300 ±500	−0.31 ±0.06	+0.62 ±0.22	2.1 ±0.2	1.65 ±0.10	2.58 ±0.05
Secondary	B9 V	+1.01 ±0.23	10400 ±500	−0.33 ±0.06	+0.68 ±0.23	2.0 ±0.2	1.62 ±0.10	2.48 ±0.05

would certainly not repeat from one event to the next because the two orbital periods are not commensurable.

7.8 Stellar rotation

As mentioned in Section 2, the observed (projected) rotational velocity of the giant component is 14.0–14.3 km s^{-1}. For synchronous rotation, its equatorial velocity would be 13.9 km s^{-1}, viewed as a projected velocity of 13.7 km s^{-1}. That value is so very close to the observed one that synchronous rotation appears extremely likely.

In the case of the B stars, synchronous rotation would give rise to a projected velocity of of 82.5 km s^{-1} for the smaller star and 86.5 km s^{-1} for the larger one. We measured the (projected) velocity as 95 km s^{-1}, but assigned an uncertainty of at least $\pm$10 km s^{-1} because the lines are broad and shallow. Moreover, during the passage of an hour (the regular exposure time) the orbital velocity of each B star alters by as much as $\sim$37 km s^{-1} if the observation occurred near conjunction (phases .25 or .75 in the inner orbit), though by only a trivial amount if observed near a node (phases .0 or .5). Although the two B-star spectra could not be measured separately if observed close to conjunction, enough blurring from their bodily velocity changes will have been included in our measurements to account for the excess between the mean measured rotational velocities and the synchronous values. It thus seems extremely likely that the two B stars are also rotationally synchronized to their orbital period.

8 EVOLUTIONARY TRACKS AND ISOCHRONE

We investigated the evolutionary history of HD 216572 by comparing the log $T_{\rm eff}$, log L values given in Table 7 for the three component stars with evolutionary tracks that had been generated for their respective masses by the publicly available software described in Pols et al. (1998); solar abundances were adopted. The computations include convective overshooting, as recommended by their authors for the range of stellar masses in question. The match with the observed HR diagram positions (Fig. 7) is tolerably satisfactory for all three stars, though the B stars do not appear as far separated in luminosity as their difference in mass would suggest; the error bars

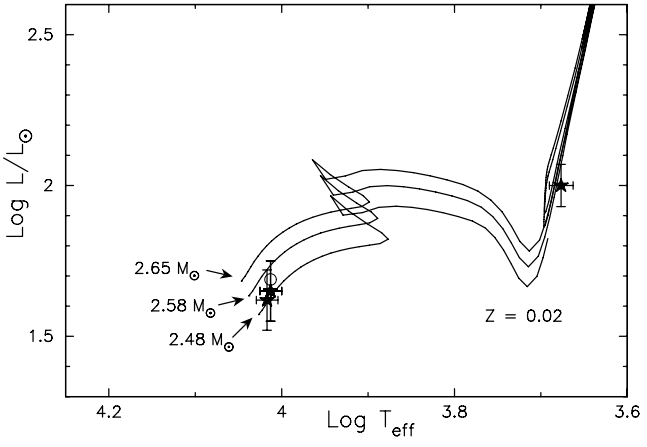

Figure 7. The positions of the three component stars in the HR diagram are compared to evolutionary tracks computed for the masses given in Table 7. Solar abundances were adopted. The open circle indicates the position corresponding to the primary B-star if it had a radius of 2.2 R$_\odot$; its error bars have been omitted for clarity. Computations used the Pols et al. (1998) package.

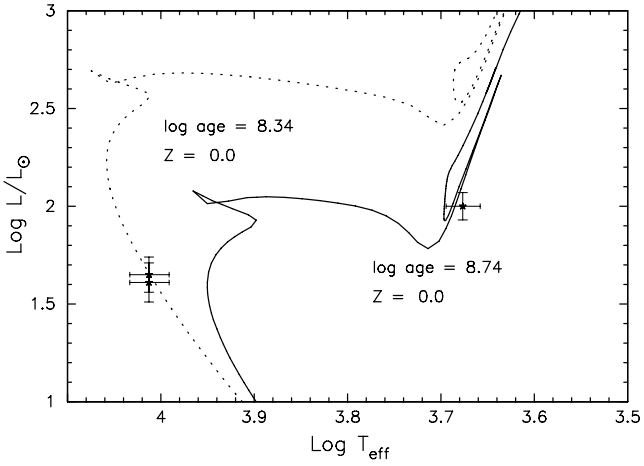

Figure 8. The positions of the three component stars in the HR diagram are compared to isochrones corresponding to an evolutionary age of 5.5 $\times$ 10^8 yr (solid line) and 2.2 $\times$ 10^8 yr (dotted line) and solar metallicity. Computations used the Pols et al. (1998) package.

of the more massive B star barely reach to its supposed evolutionary track. There is, however, a formal uncertainty of $\pm$0.01 M$_\odot$ in the mass ratio of the B stars, and the actual differences in their masses could be smaller than is represented by the q value in Table 5. As mentioned in Section 7.2.2, a difference in luminosity that would correspond exactly with the difference in mass as given in Table 5 is not borne out by the measured equivalent widths of the 48 pairs of Mg II lines.

When we study the possible isochrones for this system the situation is rather puzzling: the evolutionary age (since the main sequence) of about 5.5 $\times$ 10^8 yr for the cool giant is some 2.5 times greater than the corresponding average age of 2.2 $\times$ 10^8 yr for the two B stars. Both isochrones are drawn in Fig. 8 to indicate the size of the discrepancy.

This somewhat unsatisfactory result may suggest that the inner system is not at present in a stable equilibrium, in which case a single isochrone is not applicable. Indeed, if (as Fig. 6 could suggest) the secondary system is actively acquiring matter from the cool giant, that will exacerbate the lack of equilibrium. There seems little scope for adjustment to any of the stellar parameters by the amounts required to match a single age descriptor that links the system *in its present state* to a plausible original one. Because the giant is nowhere near filling its Roche lobe, it is improbable that recent mass transfer is causing the hot pair to appear more luminous than would now correspond to their initial masses. While that does not preclude past episodes of mass transfer, the fact that the cool giant is evidently rotating synchronously does make it somewhat unlikely.

9 CHROMOSPHERIC EMISSION

The emission which shows in some, but not all, spectra of HD 216572 is too weak for detection by general chromospheric-emission surveys. Its presence is confused both by the rather strong IS K line and by the broad, moving profiles of the K lines in the two B stars (see Fig. 3). While spurious emission-like features could arise as a consequence of chromospheric emission in the K-line core of the surrogate giant that is not matched in the primary star, the intrinsic emission in the surrogate giant used here (λ Peg) is in fact weak, and since only 25 per cent of the intensity of the surrogate

spectrum was subtracted any impact from that source will not have been noticeable here; furthermore, it would have been present in all spectra and not just in some of them.

That emission is seen is not surprising, given that the orbit for that star has a period of only 54.7 d and – what may be more relevant – the giant rotates with that period. The giant component of 93 Leo, which shows quite pronounced chromospheric Ca II emission (Griffin & Griffin 2004), has a rotational velocity of 7.8 km s^{-1} (and is possibly not in synchronous rotation); the giant in HD 216572 has comparable temperature and luminosity, so what *is* surprising is that the emission arising from it is not stronger than it is. Other composite-spectrum binaries which have $P \lesssim 120$ d and which display quite strong chromospheric emission include HR 958 and HR 2030. Both primary stars of those systems are K0 II giants, whereas HD 223971 ($P = 50$ d) also shows quite strong emission, but its cool primary appears to be a G8 III star. On the other hand HR 5983, HD 201270, HD 69479, α Equ, 3 Boo and *o* Leo, all of which also have $P \lesssim 120$ d, show no chromospheric emission that is evident against the spectrum of the secondary component. The cool components in this last category are all normal G-type giants. It is difficult to judge, from that somewhat ambiguous evidence, whether the emission is related to the luminosity of the giant, by the speed and/or synchronization of rotation or by some quite different parameter(s).

Because the emission is rather broad and the stellar line-profiles are not only broad too but also somewhat noisy, its impact may not always be obvious visually. We make this point as a caution regarding the more general possibility of chromospheric contamination in (weak) K-line profiles.

9.1 Concluding remarks

This analysis of HD 216572 has produced a remarkably consistent set of parameters for the three components, notwithstanding the relative faintness of the system and the small aperture of the telescope which was the prime source of the spectroscopy. By isolating the spectra of the two very similar B9 dwarfs which comprise the short-period system we could make RV measurements on all the spectra that had been observed at phases of adequate velocity separation. We incorporated the 48 measurements made at the Mg II λ4481 Å line into a triple-lined orbit solution, and showed thereby that the B stars differ in mass by 4 per cent.

Subtraction of the contributions of the cool giant from the combined photometry revealed narrow and slightly unequal eclipse light curves, about 0.2 mag deep, for the inner pair. Although the orbit has a period of under 1.2 d and the surfaces of the stars are separated by only the sum of their radii, the light curves do not show marked effects of ellipticity or reflection such as might be expected in those circumstances, and our analysis did not include such effects. By removing the known photometric variations in the inner system, we could examine more closely any evidence for a grazing eclipse of that system by the primary. None appeared, but what we found instead was possible evidence for an accretion column which may cause the secondary system to appear dimmed as it passes behind it a few days before the actual date of conjunction.

However, the analysis has also revealed a substantial lack of agreement with any reasonable theoretical isochrone. It would be very interesting to acquire much more detailed observational material for this system in spectroscopy, photometry and direct imaging, not only to understand the physics of the system better but also to understand at what level the generalizations and assumptions which are unavoidable in work of this nature actually cease to be valid.

ACKNOWLEDGMENTS

We are very grateful to the DAO for the many opportunities to observe spectra of this star at high dispersion, and to the Geneva Observatory, Palomar Observatory, the DAO and ESO for RFG's radial-velocity observing time; we owe our gratitude to PPARC and to its predecessor SERC for defraying the costs of all the pre-2002 observing runs which have contributed data used in this paper. We have benefited from discussions with Peter Eggleton, we are grateful to Bob Wilson for his interest in this triple system, and we thank the referee (Barry Smalley) for constructive input. REMG offers special thanks to the DAO for the use of its PDS, and acknowledges with pleasure the visitor privileges offered by that Observatory. This research has made use of the SIMBAD data base, operated at CDS, Strasbourg, France.

REFERENCES

Abt H. A., 1985, ApJS, 59, 95
Adelman S. J., Pintado O. I., Nieva F., Rayle K. E., Sanders S. E., Jr, 2002, A&A, 392, 1031
Aitken R. G., 1932, New General Catalogue of Double Stars Within 120° of the North Pole. Carnegie Institution of Washington, Washington, DC, 2, 1416
Andersen J., 1991, A&AR, 3, 91
Baranne A., Mayor M, Poncet J. L., 1979, Vistas. Astron., 23, 279
Bassett E. E., 1978, Observatory, 98, 122
Benedict G. F. et al., 2002, AJ, 124, 1695
Blanco V., Nassau J. J., Stock J., Wehlau W., 1955, ApJ, 121, 637
Cannon A. J., Pickering E. C., 1924, Ann. Harvard Coll. Obs., 99, 174
ESA, 1997, The *Hipparcos* and *Tycho* Catalogues, ESA SP-1200. ESA Publications Division, Noordwijk
Fekel F. C., Tomkin J., 1982, ApJ, 263, 289
Fletcher J. M., Harris H. C., McClure R. D., Scarfe C. D., 1982, PASP, 94, 1017
Flower P. J., 1996, ApJ, 469, 355
Gray R. O., Garrison R. F., 1987, ApJS, 65, 581
Grenier S. et al., 1999, A&AS, 137, 451
Griffin R. F., 1967, ApJ, 148, 465
Griffin R. F., 1969, MNRAS, 145, 163
Griffin R. F., 1990, JA&A, 11, 491
Griffin R. F., 2001, Observatory, 121, 315
Griffin R. F., 2006, Observatory, 126, 338
Griffin R. & R., 1979, A Photometric Atlas of the Spectrum of Procyon. R. & R. Griffin, Cambridge
Griffin R. & R., 1986, JA&A, 7, 195
Griffin R. E. M., Griffin R. F., 2004, MNRAS, 350, 685
Griffin R. F., Gunn J. E., 1974, ApJ, 191, 545
Griffin R. E. M., Griffin R. F., Stickland D. J., 2006, MNRAS, 373, 1351
Høg E. et al., 2000, A&A, 355, L27
Kazarovets A. V., Samus S. S., Durlevich O. V., Frolov M. S., Antipin S. V., Kireeva N. N., Pastukhova E. N., 1999, Inf. Bull. Variable Stars, No. 4659, 24
Keenan P. C., Barnbaum C., 1999, ApJ, 518, 859
Keenan P. C., McNeil R. C., 1989, ApJS, 71, 245
Kuhi L. V., 1963, PASP, 75, 448
Lehmann-Filhés R., 1894, AN, 136, 17
Mazeh T., 1990, AJ, 99, 675
Mozurkewich D. et al., 2003, AJ, 126, 2502
Pols O. R., Schröder K.-P., Hurley J. R., Tout C. A., Eggleton P. P., 1998, MNRAS, 298, 525
Schlesinger F. C., 1914, Publ. Allegheny Obs., 3, 173
Schmidt-Kaler T., 1982, in Schaifers K., Voigt H. H., eds, Landolt-Börnstein, New Series, Gp. 6, Vol. 2b. Springer-Verlag, Berlin, Table 4.1
Smith G., 1998, A&A, 339, 531
Slettebak A., Nassau J. J., 1959, ApJ, 129, 88

Sterne T. E., 1941, Proc. US Natl Acad. Sci., 26, 175
Struve F. G. W., 1827, Catalogus Novus Stellarum Duplicium et Multiplicium. Typographia Academia, Dorpat, p. 74
Struve F. G. W., 1837, Stellarum Duplicium et Multiplicium Mensurae Micrometricae per Magnum Fraunhoferi Tubum Annis a 1824 ad 1837 in Specula Dorpatensis. Typographia Academia, Petropolis, p. 164
Udry S., Mayor M., Queloz D., 1999, in Hearnshaw J. B., Scarfe C. D., eds, ASP Conf. Ser. Vol. 185, Precise Stellar Radial Velocities. Astron. Soc. Pac., San Francisco, p. 367
van Hamme W., 1993, AJ, 106, 2096
Vrancken M., Hensberge H., David M., Verschueren W., 1997, A&A, 320, 878
Willstrop R. V., 1965, Mem. R. Astron. Soc., 69, 83

This paper has been typeset from a TEX/LATEX file prepared by the authors.